Optimised Condition Catalytic Upgrading of Agbabu Bitumen in the Presence of Rice Husks

Yunusa Mohammed Oseni [1, 2], **Umar Omeiza Aroke** [2], **Baba Jibril Yakubu** [3]

[1] *Bayero University Kano*
Nigeria Gwarzo Road, P. M. B. 3011, Kano, Nigeria

[2] *Abubakar Tafawa Balewa University*
Dass road, P. M. B. 0248, Bauchi, Nigeria

[3] *Ahmadu Bello University*
Zaria, 810211, Nigeria

DOI: 10.22178/pos.103-11

LCC Subject Category: GV1100-1150.9

Received 21.03.2024
Accepted 25.04.2024
Published online 30.04.2024

Corresponding Author:
Yunusa M. Oseni
yunusamohammedoseni@gmail.com
ymoseni.cpe@buk.edu.ng

Abstract. In this study, the optimisation of bitumen collected from Agbabu Ondo State, Nigeria, was upgraded in the presence of rice husks in a nitrogen environment using a 100 ml autoclave batch reactor with the aid of the design expert software. Response surface methodology (*RSM*) was used to determine the optimum conditions for the bitumen upgrading in the presence of rice husks using the Box-Behnken Designed Experiment (BBD). Three mesoporous aluminosilicate catalysts (NiMo/ZSM-5, CoMo/HZSM-5 and Mo/HZSM-5) were used to upgrade the bitumen at the obtained optimised point. The bitumen sample was characterised by saturates (53.48 wt.%), aromatics (12.84 wt.%), resins (15.37 wt.%), asphaltenes (8.86 wt.%) and an initial viscosity of 86.78 Pa.s, API gravity of 7.87 ° and density of 1.0153 kg/l. The GC-MS result revealed that there were 42 chemical compounds present in the raw bitumen. The XRF result for the rice husks revealed that the silica to Alumina (SiO_2/Al_2O_3) ratio was 11.89:1. RSM optimisation of the experimental runs with the autoclave reactor gave an optimum condition (Temperature of 345.716 °C, Reaction time of 30 min, and Rice husks of 1.0 wt.%) without employing any of the three mesoporous aluminosilicate catalysts. The responses obtained for the upgraded oil were viscosity 8.34 Pa.s, API gravity 24.520 °, residue yield 22.39 w/w% and light oil yield 50.064 w/w%. The experimental run with NiMo/ZSM-5 catalyst at the optimum conditions was observed to be more effective in the catalytic thermal cracking of the bitumen upgrading process, as the light oil yield was 70.42 w/w%, viscosity of 2.060 Pa.s, API gravity of 29.826° and residue yield of 10.66 w/w% compared to what was obtained from CoMo/HZSM-5 and Mo/HZSM-5 mesoporous aluminosilicate catalysts. The FT-IR and GC-MS of the upgraded Agbabu bitumen testified that the level of upgrade of the bituminous oil was satisfactory as the raw Agbabu bitumen had an initial viscosity of 86.780 Pa.s, API gravity of 7.87 ° and density of 1.0153 kg/l in which all the initial core properties of the bitumen have shifted satisfactorily after the bitumen upgrade to produce light oil that fell within the acceptable range of refinery feedstock specifications for refining processes in the vacuum distillation unit (VDU).

Keywords: Heavy Oil; Bitumen; Bitumen Upgrading; Rice Husks; Mesoporous Aluminosilicate Catalysts

INTRODUCTION

The growing global demands for fossil fuels due to the worldwide increase in human population and technological advancement has led to the fast depletion of conventional crude oil and thus the need to seek and adopt a viable means to which the provision for the fossil fuels demands could be sustained, gave rise to the keen interest by researchers and oil industry based researchers to look onto unconventional oils – mainly heavy oils, extra-heavy oils and bitumen as an alternative source for the fossil fuels provision. Over half of the world's oil reserves are recoverable oils such as heavy oil, extra heavy oil, bitumen, etc. However, there are many challenges governing the recovery and using these oil sources in regular refinery routes to process them into valuable fuels. Figure 1 shows the world oil reserves [1].

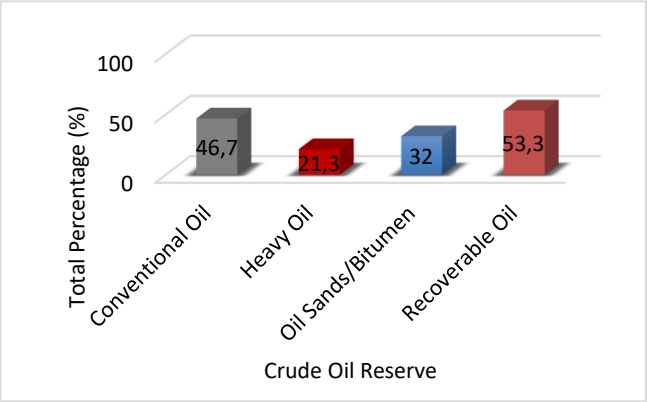

Figure 1 –Total World Oil Reserve

Bitumen constitutes mainly hydrocarbons possessing low hydrogen-to-carbon ratio (H/C) with high molecular weights that result in high boiling points, and most bitumen have a typical carbon atom greater than 15 in their molecular structures. Their components can be classified as saturates, aromatics, resins, and asphaltenes (SARA), concerning their polarizability and polarity [2]. The bitumen is characterised and determined mainly by the amount of asphaltenes followed by resins present in the bitumen. Thus, the viscosity of the bitumen is a function of asphaltenes content in the bitumen such that the greater the volume percentage of the asphaltenes, the greater the viscosity of the bitumen. The bitumen has an average range of values for H/C (1.0–1.2), density (1.1–1.20 Kg/l), and at an ambient condition of solubility (19–24 Mpa). Natural bitumen has API gravity in the range of 7–14°, high viscosity in the range of 5–100 Pa.s, and high content of sulphur, oxygen, nitrogen, and heavy metals such as nickel and vanadium. The structure of bitumen is condensed polynuclear aromatic rings containing branched chains of the alkyl group. The number of these polynuclear atomic rings may be present in the proportion ranging from 6–15 in the case of asphaltenes [2, 3].

The combination of bitumen with other resources, such as catalysts and biomass after bitumen production, has been growing in interest by researchers and oil industry-based researchers globally for upgrading the bitumen to light oil. Biomass is a renewable, carbon iv oxide (CO_2) free energy source with low sulphur content. It can be mixed with bitumen over a mesoporous aluminosilicate catalyst for chemical modification to produce light oil [4]. Rice husks are biomass with low density and less commercial interest by the public, so their handling and transportation become problematic, creating disposal and serious environmental problems. Thus, the need to properly dispose of rice husks in waste utilisation gave rise to its usage in bitumen upgrading for fossil fuel supply and sustainability [5].

Lots of heavy oil/bitumen upgrading methods used were observed as remarked that the viscosity of the upgraded heavy oils or bitumens seems to backslide as time goes by, resulting in greater viscosities as there is the presence of heteroatoms such as oxygen, nitrogen and sulphur and regeneration of free radicals. Thermal upgrading of heavy oil/bitumen in the presence of a catalyst and biomass is believed to show a notable promise in heavy oil/bitumen upgrading if exploited as with the noteworthy accomplishment obtained from thermal upgrading with catalyst alone [5]. In this context, catalytic thermal cracking of natural bitumen with rice husks to produce a stabilised light oil using a mesoporous aluminosilicate catalyst at optimum conditions will be investigated, hence this study. In this light, this research work aims to upgrade the natural bitumen collected from the Agbabu Ondo State of Nigeria at optimum conditions (optimum conditions obtained first from upgrading the Agbabu bitumen using rice husks only without employing any nano-catalysts at the initial stage of the bitumen upgrade to find the optimum conditions

for upgrade)[1] over three separate mesoporous aluminosilicate catalysts (NiMo/ZSM-5, Co-Mo/HZSM-5, and Mo/HZSM-5) to see the effects of the upgrade by a combination of rice husks and catalysts at different experimental runs with the ambition to find a mean to ensure a constant future fuel supply and away of proper disposal/utilisation of rice husks waste.

METHOD

Materials/Chemicals. Bitumen was collected from Agbabu bituminous field, Ondo State, Nigeria. Table 1 lists the properties of the bitumen - different laboratories have conducted and collated analyses of the bituminous oil.

Table 1 – Agbabu, Ondo State Bitumen

Parameter	Value
Viscosity @ 70 °C (Pa.s)	86.780
Density @ 60 °C (Kg/l)	1.0153
API gravity (°)	7.870
Sulfur (wt.%)	6.33
Hydrogen to Carbon (H/C) ratio	1.19
Water in Crude (Karl Fisher ASTM D4928);	
Initial Crude	23.94
Dehydrated Crude	3.26
Micro-Elemental Composition (%);	
Carbon (C)	76.64
Hydrogen (H)	7.67
Nitrogen (N)	0.25
Sulfur (S)	4.51
Oxygen (O)	37.1
Metal Composition (ppm)	
Nickel (Ni)	800
Vanadium (V)	2000
SARA Composition (wt.%);	
Saturates	53.48
Aromatics	12.84
Resins	15.37
Asphaltenes	8.86

Notes: Analyses conducted at different laboratories and collated

The rice husks were collected from a local rice mill in Kano State, Nigeria. They were dried in an oven to ensure minimal moisture content, and their physicochemical properties were characterised.

The following chemicals were used: Toluene (Sigma-Aldrich), n-Hexane (Fisher Scientific), Nitrogen (99.82%), Silica gel, and Attapulgus clay were obtained from a local supplier.

The three catalysts employed were mesoporous aluminosilicate catalysts: NiMo/ZSM-5, CoMo/HZSM-5, and Mo/HZSM-5. Each catalyst was characterised.

Characterisation of Raw Bitumen, Rice Husks and Mesoporous Aluminosilicate Catalysts. The raw bitumen (Agbabu bitumen), rice husks and mesoporous aluminosilicate catalysts were characterised, and their physiochemical properties were recorded under the following headings.

Characterisation of Raw Agbabu Bitumen. Characterisations (viscosity, API gravity, density, etc.) of the Agbabu bitumen were carried out to determine the properties of the raw bitumen, as shown in Table 1. FT-IR, GC-MS, XRF, and micro elemental analysis were also carried out to further determine the raw bitumen's properties.

Characterisation of Rice Husks. The rice husk was collected from a local rice mill in Kano State, Tofa Local Government of Nigeria. Characterisations such as the oxide and elemental analysis were carried out to determine the properties of the rice husks using XRF and XRD machines.

Characterisation of Modified Aluminosilicate Catalysts. The three mesoporous aluminosilicate catalysts (NiMo/ZSM-5, CoMo/HZSM-5, and Mo/HZSM-5) employed in the heavy oil upgrade were characterised using X-ray powder diffraction (XRD), scanning electron microscope (SEM), and BET analysis machines.

Optimisation of Agbabu Bitumen Upgrading in the Presence of Rice Husks. Using response surface methodology (RSM), the Agbabu bitumen was optimised to obtain the optimum conditions. The Box-Behnken Design experiment was used as the design template for the optimisation reaction experiment.

Catalytic Thermal Cracking Experiment at the Optimum Conditions. Now, applying the optimum conditions obtained from the optimisation of Agbabu bitumen for the upgrade, the bitumen catalytic thermal cracking experiment was carried out in an autoclave 100 ml batch reactor. Explicitly, a total of 50 g of (Raw Agbabu bitumen + 1.0 wt.% rice husks + 0.5 wt.% catalyst) amounting to 49.25 g of raw bitumen, 0.5 g of rice husks and 0.25 g of mesoporous aluminosilicate catalyst were mixed in the reactor, indicat-

[1] The optimisation of Agbabu bitumen in the Presence of Rice Husks was performed to obtain the optimum condition

ing a 0.0051 catalyst-to-oil (C/O) ratio for the bituminous catalytic thermal experiment.

The reactor was closed but with the gas exit valve opened (and later, the gas exit valve was closed to air tighten the reactor before the reaction), then nitrogen gas was passed through the reactor and made to exit through the gas exit valve of the reactor for few seconds before air tighten of the reactor to drive away any trapped gases in the reactor. The reactor was pressurised with nitrogen gas at a pressure of 6 bar, followed by a leakage test before the reaction. The stirrer was set at a rotational speed of 500 rpm, and the reaction time began nearly 120 min after the heating element of the autoclave reactor was switched on. The reaction temperature was ensured to be stabilised at 345.716 °C. The reaction was permitted for 30 min as setup, after which the reactor system was automatically switched off, and the reactor was allowed to cool over time. The gas was vented out and trapped through a gas board analyser (Gasboard 3100P), and the resulting light oil was separated from the residue oil. The light oil and the residue oil were weighed separately - the light crude was measured for viscosity and API gravity. Figure 2 shows the experimental method and analytical scheme of bitumen upgrading.

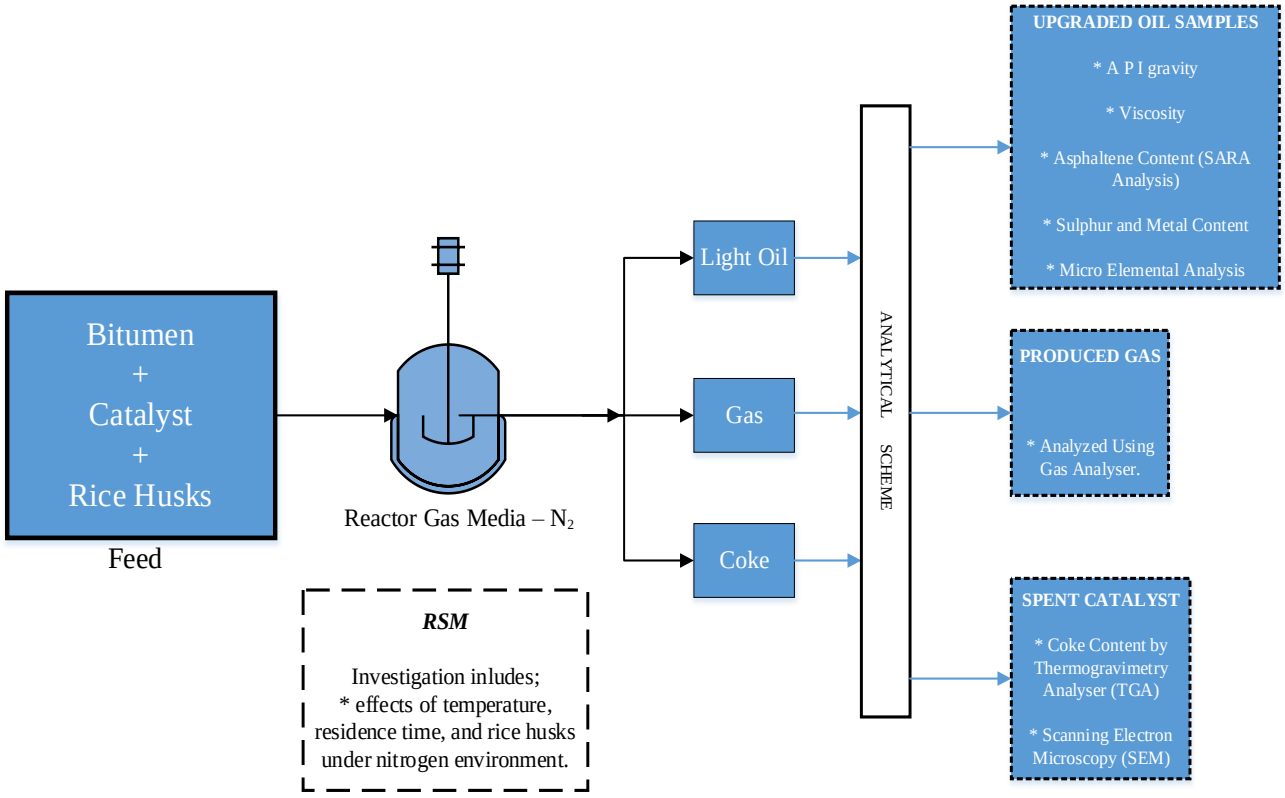

Figure 2 – Experimental Method and Analytical Scheme of Bitumen Upgrading

Four experimental runs were carried out by employing three different mesoporous aluminosilicate catalysts and optimal crude (without catalyst) to validate the optimum conditions known as the validation point. In this experiment, 0.5 wt.% mesoporous aluminosilicate catalysts of NiMo/ZSM-5, CoMo/HZSM-5 and Mo/HZSM-5 were employed respectively at a total weight of 50 g feed to further upgrade the bituminous oil at the optimum conditions (temperature of 345.716 ^{0}C, reaction time of 30.0 minutes and 1.0 wt.% of rice husks) to ascertain the effects of each catalyst on the optimised upgraded Agbabu bitumen to obtain optimised catalytically upgraded Agbabu bitumen. The composition of the four experimental runs at optimum conditions are:

1. Raw Bitumen + 1.0 wt.% Rice Husks (Optimal Crude).

2. Raw Bitumen + 1.0 wt.% Rice Husks + 0.5 wt.% NiMo/ZSM-5 (NiMo/ZSM-5 Catalyzed Crude).

3. Raw Bitumen + 1.0 wt.% Rice Husks + 0.5 wt.% CoMo/HZSM-5 (CoMo/HZSM-5 Catalyzed Crude).

4. Raw Bitumen + 1.0 wt.% Rice Husks + 0.5 wt.% Mo/HZSM-5 (Mo/HZSM-5 Catalyzed Crude).

RESULTS AND DISCUSSIONS

Physicochemical Properties of Raw Agbabu Bitumen. The physicochemical properties of the Agbabu bitumen are shown in Table 1.

FT-IR Analysis of Raw Agbabu Bitumen. This was performed to determine the functional group compositions of the Agbabu bitumen, as shown in Figure 3.

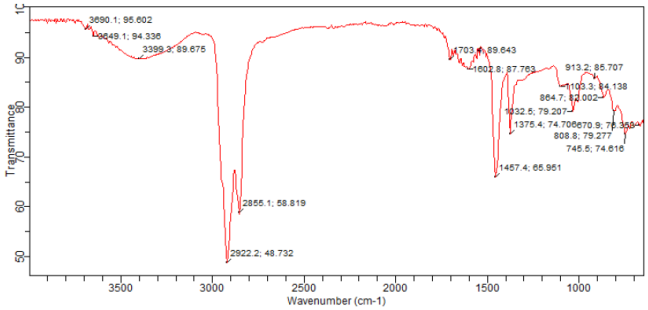

Figure 3 – FT-IR Spectrum of Raw Agbabu Bitumen

The FT-IR result obtained for the raw Agbabu bitumen in Figure 3 revealed that there were 3 broad peaks, 3690.1 cm^{-1}, 3649.1 cm^{-1}, and 3399.3 cm^{-1} observed in the range of 3700–3400 cm^{-1} absorption bands. This range (3700–3400 cm^{-1}) of absorption bands indicates hydrogen bonding and confirms the existence of hydrate (H_2O), hydroxyl (–OH), ammonium, or amino, phenolic, alcoholic and carboxylic compounds. The 3399.3 cm^{-1} absorption band is assigned to the hydrogen-bonded O–H group (intermolecular H bond) in phenolic, alcoholic, and carboxylic acid compounds in the asphaltenes [6]. The two intense peaks (2855.1 cm^{-1} and 2922.2 cm^{-1}) are assigned to –CH stretching bands for long-chain linear aliphatic compounds [7]. There were no observable peaks between the range (2800–1800 cm^{-1}) of absorption bands. But this absorption range is assigned to different functional groups; peaks between 2700 cm^{-1} and 2800 cm^{-1} are specific to aldehydes; (2500–2000 cm^{-1}) are the triple (C≡C) bond region and transition metal carbonyls. The peak 1703.4 cm^{-1} indicated simple amides, carbonyl compounds like ketones, aldehydes, esters or carboxylates functional group [8]. The medium peak 1602.8 cm^{-1} indicated the presence of double bond (C = C) stretching or olefinic compounds. 1457.4 cm^{-1} and 1375.4 cm^{-1} peaks were attributed to the bending vibration of C–H in methylene and methyl, respectively. The peak observed at 1103.3 cm^{-1} band was likely for esters linkages in asphaltene molecules. The band attributed to 1032.5 cm^{-1} was assigned S=O in alkane-substituted sulfoxides and also ester linkages present in asphaltene molecules, vinyl–related compounds found in resins, C-H bending in aromatics and C-O-C in mixed ethers [9]. The 913.2 cm^{-1} band was assigned to aliphatic fluoro compounds, C-F stretch, vinyl C-H out-of-plane bend and cyclohexane ring vibrations. The range of bands (870–730 cm^{-1}) was assigned to aromatic C-H out-of-plane bend [8].

GC-MS Analysis of Raw Agbabu Bitumen. GC-MS of the raw Agbabu bitumen was carried out to determine the chemical compounds present in the raw Agbabu bitumen. Asphaltenes, as one of the significant characteristics of heavy oil or bitumen, are non-volatile complex compounds consisting of different polymeric compounds with higher molecular weights. They are challenging to detect and analyse by merely GC-MS methods as GC-MS works on a chemical compound's volatility principle. Thus, in the GC-MS spectra of the raw bitumen and upgraded heavy oil or bitumen in this work, the GC-MS machine was able to detect and analyse aliphatics (saturates, cycloalkanes, alkenes, cycloalkenes, etc.), aromatic compounds, resins (low to no volatile compounds or semi-volatile), ester and polar compounds. There are 42 chemical compounds present in the raw bitumen obtained from the GC-MS spectra, as shown in Table 2.

The raw bitumen shown in Table 2 contains aliphatic compounds. These aliphatic compounds consist mainly of different C_8 – C_{20} paraffinic hydrocarbons (saturates), alicyclic compounds in small amounts, and alkene. However, not all the chemical compounds present in GC-MS spectra could be identified, thus showing the nature and complexity of those that could not be determined.

The aromatic compounds in the raw bitumen shown in Table 2 consist of monochromatic, polycyclic aromatic hydrocarbons and heterocyclic hydrocarbons containing sulphur and nitrogen. Pyrene, naphthalene, biphenyl, anthracene, indene, and phenanthrene derivatives are included in polycyclic aromatic hydrocarbons. While heterocyclic hydrocarbons containing sulphur consist of mainly thiophenes derivatives, the heterocyclic hydrocarbons containing nitrogen contain derivatives such as indole, pyridine, quinolone, etc. [10].

Table 2 – Chemical Composition of Raw Agbabu Bitumen from the GC-MS Analysis

No	Chemical Compound	CAS No	Mol. Formula	Mol. Wt. (g/mol)	Nature of Compounds
1	Vestitenone	069401-36-1	$C_{12}H_{18}O$	178.27	Aromatic
2	4-Methylundecane	002980-69-0	$C_{12}H_{26}$	170.34	Saturate
3	Undecane	001120-21-4	$C_{11}H_{24}$	156.31	Saturate
4	2-Methyltridecane	001560-96-9	$C_{14}H_{30}$	198.39	Saturate
5	Tridecane	000629-50-5	$C_{13}H_{26}$	184.36	Saturate
6	Tetradecane	000629-59-4	$C_{14}H_{30}$	198.39	Saturate
7	Spiro[2,4,5,6,7,7a-hexahydro-2-oxo-4,4,7a trimethylbenzofuran]-7,2'-(oxirane)	1000197-10-9	$C_{12}H_6O_3$	208.25	Aromatic
8	Sclareoloxide	051553-92-4	$C_{18}H_{30}O$	262.43	Resin
9	Oxalic acid, 6-ethyloct-3-yl hexyl ester	1000309-34-4	$C_{18}H_{34}O_4$	314.50	Aromatic
10	4-Ethyloctane	015869-86-0	$C_{10}H_{22}$	142.28	Saturate
11	2,6-dimethyloctane	002051-30-1	$C_{10}H_{22}$	142.28	Saturate
12	Methyl 2-oxo-5,6,7,8-tetrahydro-1H-quinoline-3-carboxylate	125031-45-0	-	-	-
13	2,4-Dimethylhexane	000589-43-5	C_8H_{18}	114.23	Saturate
14	Ethyl 5-(furan-2-yl)-1,2-oxazole-3-carboxylate	33545-40-3	$C_{10}H_9O_4$	207.18	Aromatic
15	E-11-Methyl-12-tetradecen-1-ol acetate	1000130-80-7	$C_{17}H_{32}O_2$	268.44	Aromatic
16	E-10-Methyl-11-tetradecen-1-ol acetate	1000130-79-0	$C_{17}H_{32}O_2$	268.44	Aromatic
17	4-Methyldodecane	006117-97-1	$C_{13}H_{28}$	184.37	Saturate
18	3-Methyldodecane	017312-57-1	$C_{13}H_{28}$	184.37	Saturate
19	Dodecane	000112-40-3	$C_{12}H_{26}$	170.33	Saturate
20	D-Homoandrostane, (5.alpha.,13.alpha.)-	054482-31-4	$C_{20}H_{34}$	274.49	Aromatic
21	2-Methyldecane	006975-98-0	$C_{11}H_{24}$	156.31	Saturate
22	2,9-Dimethyldecane	001002-17-1	$C_{12}H_{26}$	170.33	Saturate
23	2,4-Dimethyldecane	002801-84-5	$C_{12}H_{26}$	170.33	Saturate
24	Decane	000124-18-5	$C_{10}H_{22}$	142.29	Saturate
25	Cyclopropane carboxamide, 2-cyclopropyl-2-methyl-N-(1-cyclopropylethyl)-	331416-19-4	$C_{13}H_{21}NO$	207.16	Aromatic
26	Cyclopentanecarboxaldehyde, 2-methyl-3-methylene-	1000154-24-0	$C_8H_{12}O$	124.18	Aromatic
27	Cyclohexene, 4-pentyl-1-(4-propylcyclohexyl)-	108067-17-0	$C_{20}H_{36}$	276.50	Saturate
28	Cyclohexene, 4-(4-ethylcyclohexyl)-1-pentyl-	301643-32-3	$C_{19}H_{34}$	262.48	Saturate
29	Androstane, (5.alpha.)-	000438-22-2	$C_{19}H_{32}$	260.46	-
30	Cyclohexanebutanoic acid,2,2-dimethyl-6-methylene-, methyl ester	081752-87-6	$C_{11}H_{18}O_2$	182.26	Aromatic
31	Cholestan-3-ol, 4,4-dimethyl-, (3.beta.,5.alpha.)-	002550-84-7	$C_{29}H_{52}O$	416.72	-
32	Carbonic acid, nonyl vinyl ester	1000383-25-6	$C_{12}H_{22}O_3$	214.30	Resin
33	Carbonic acid, eicosyl vinyl ester	1000382-54-3	$C_{23}H_{44}O_3$	368.60	Resin
34	Androstane-2,11-dione, (5.alpha.)-	001449-57-6	$C_{19}H_{28}O_2$	288.42	-
35	3-Trifluoroacetoxypentadecane	1000245-47-8	$C_{17}H_{31}F_3O_3$	324.40	-
36	2-Bromononane	002216-35-5	$C_9H_{19}Br$	207.16	Saturate
37	1H-Indene, 5-butyl-6-hexyloctahydro-	055044-36-5	$C_{19}H_{36}$	264.49	Aromatic
38	1H-Indene, 2-butyl-5-hexyloctahydro-	055044-33-2	$C_{19}H_{36}$	264.49	Aromatic
39	10-Methylnonadecane	056862-62-5	$C_{20}H_{42}$	282.56	Saturate
40	1,1,6-trimethyl-3-methylene-2-(3,6,9,13-tetramethyl-6-ethenye-10,14-dimethylene-pentadec-4-enyl)cyclohexane	1000373-94-5	$C_{33}H_{56}$	452.80	Aromatic
41	1(3H)-Isobenzofuranone,6,7-dimethoxy-3-[2-(2-methoxyphenyl)-2-oxoethyl]-	1000350-76-1	$C_{19}H_{18}O_6$	342.34	Aromatic
42	(1S,4aS,4bS,7S,8aS,10aS)-7-Isopropyl-1,4a-dimethyltetradecahydrophenanthrene	002221-95-6	$C_{19}H_{34}$	262.48	Saturate

The ester compounds present in the raw bitumen in Table 2 contain furan, aldehyde, ketone acid, etc – oxygen-containing compounds. Some of these ester compounds also contain aromatic groups containing sulphur and nitrogen and are called aromatics. Thus, the nature of chemical compounds present in Table 2 was only identified as saturate, aromatic, and resin, as the as-

phaltenes in the raw bitumen cannot be detected by merely direct GC-MS spectrum due to the complex nature of asphaltenes. Figure 4 shows the GC-MS spectra for the raw Agbabu bitumen.

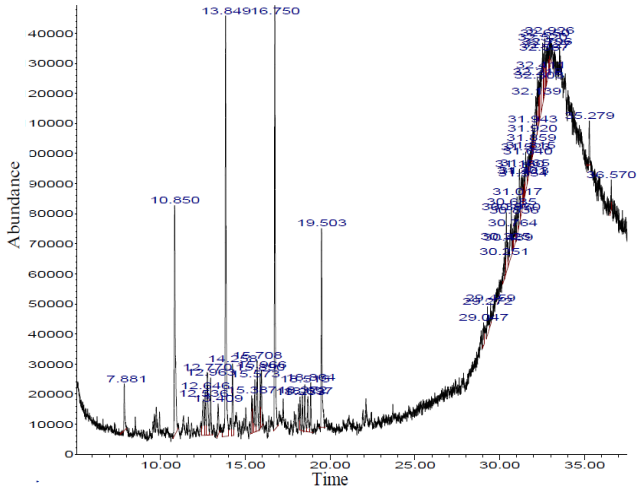

Figure 4 –GC-MS Spectrum for Raw Agbabu Bitumen

X-ray Florescence (XRF) Analysis of the Rice Husks. XRF analysis for the rice husks was performed to know the composition of the minerals in the rice husks. The elemental and oxide composition presented in Table 3 shows that the rice husks consist mainly of silica and silica oxide, with metallic oxides such as Fe_2O_3, MnO, ZnO and TiO_2 present as minor mineral compositions.

Silica and Alumina and their oxides are the main mineral compositions for the heavy oil upgrade as they support the mesoporous aluminosilicate catalysts. From Table 3, the oxide of silica (SiO_2) is 47.80 w/w%, and that of Alumina (Al_2O_3) is 6.82 w/w%.

Table 3 – XRF Analysis of Rice Husks

Oxide Composition	Value (w/w%)	Elemental Composition	Value (w/w%)
SiO_2	47.80	Si	22.35
P_2O_5	13.71	P	5.98
K_2O	12.48	K	10.36
MgO	7.20	Mg	4.40
Al_2O_3	6.82	Al	3.61
SO_3	4.93	S	1.97
CaO	2.80	Ca	2.00
Fe_2O_3	1.52	Fe	1.07
TiO_2	0.64	Ti	0.39
MnO	0.34	Mn	0.27
Rb_2O	0.11	Rb	0.10
ZnO	0.10	Zn	0.08
ZrO_2	0.08	Zr	0.06

At the same time, for elemental composition, silicon (Si) is 22.35 w/w%, and that of aluminium is 3.61 w/w% for the rice husks, which is an indication of an excellent precursor to the aluminosilicate catalysts. Thus, the XRF result for the rice husks revealed that the silica to Alumina (SiO_2/Al_2O_3) ratio is 11.89:1, and the silicon to aluminium (Si/Al) ratio is 5.95:1.

X-ray Diffraction (XRD) Analysis of the Rice Husks. X-ray Diffraction (XRD) analysis of the rice husks was performed to determine the silica and alumina phase of the rice husks sample. It was scanned by an X-ray diffractometer using CuKα radiation at 40 mA/45 kV and λ = 1.5406 Å, PSD length [2θ] of 3.35°, scan step time [s] of 29.07 sec., and scan position [2θ] at an angle/position from 5–78°. Figure 5 shows the XRD pattern of the rice husks.

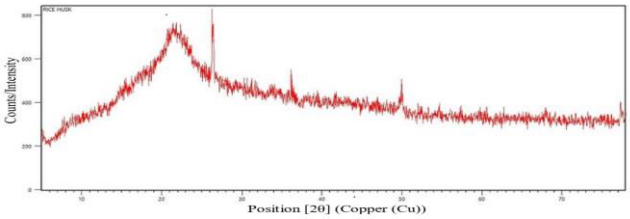

Figure 5 – X-Ray Diffraction Spectrum of Rice Husks

According to JCPDS Card Number 021-1272 of rice husks XRD pattern, the rice husks have mainly silicon (Si) in the form of SiO_2 and is indicating the Si is in amorphous form due to the broad peak on 2θ at an angle of 22°. The following three sharp prominent peaks observed on the XRD spectrum 2θ at an angle of 25.5°, 36° and 49.5° show the presence of cristobalite (SiO_2) as the only crystalline phase present in the rice husks sample. The X-ray diffractometer pattern of the rice husks also conforms to what is obtainable in the literature [11].

XRD Analysis of the Modified Aluminosilicate Catalysts. XRD analysis of the three modified aluminosilicate catalysts was carried out to determine the phase composition of the aluminosilicate catalysts. Figure 6 shows the XRD patterns of the three aluminosilicate catalysts.

The three synthesised aluminosilicate catalysts displayed peaks along the axis 2θ at an angle of 7.2°, 8.5°, 23.1°, 26° and 27.6°, which correspond to [011], [020], [051], [332], and [343] planes respectively.

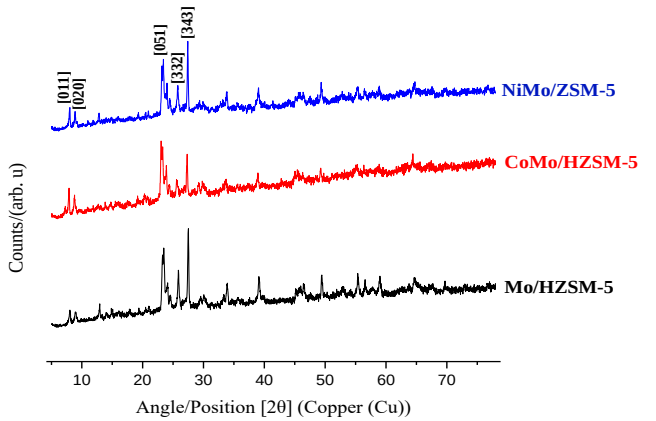

Figure 6 – X-Ray Powder Diffraction (XRD) Patterns of the Mesoporous Aluminosilicate Catalysts

The XRD patterns of all the aluminosilicate catalysts showed the characteristics of diffraction peaks of the mordenite framework inverted (MFI) crystalline structure, confirming the formation of ZSM-5 and HZSM-5 catalysts. Furthermore, the intensities of the peaks in the three aluminosilicate catalysts, as observed, are very similar, an indication that the gel used in the synthesis of the aluminosilicate catalysts did not affect the crystalline structure of the synthesised ZSM-5 and HZSM-5 catalysts [12, 13].

SEM Analysis of the Modified Aluminosilicate Catalysts. The three micrograph images (a), (b), and (c) of the aluminosilicate catalyst shown in Figure 7 show the presence of particles with agglomerated, well-defined, varied morphology. Thus providing good evidence that implies mesoporous heterogeneous surface morphology with a surface area of 705-809 m^2/g and pore volume of 0.75-0.87 cm^3/g, as evident in the BET analysis (Table 4) [14].

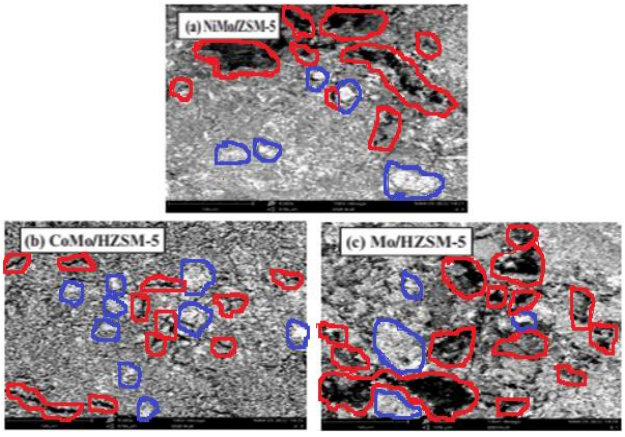

Figure 7 – SEM Micrographs of the Modified Aluminosilicate Catalysts (NiMo/ZSM-5, CoMo/HZSM-5, & Mo/HZSM-5).

The dark parts or patches on the SEM images are the pores of each catalyst, while the white spots are the solid materials of the catalyst. The catalyst becomes poisoned and deactivated when the pores are too large to accommodate the heavy crude oil's bulky molecules [13].

Table 4 – BET Properties of Mesoporous Aluminosilicate Catalysts

Catalyst	Surface area (m^2/g)	APD (nm)	Pore Volume (cm^3/g)
NiMo/ZSM-5	809	3.8	0.87
CoMo/HZSM-5	705	3.4	0.63
Mo/HZSM-5	798	3.6	0.75

Thus, mesoporous catalysts with larger pore volumes and active sites were used to upgrade bitumen.

BET Analysis of the Modified Aluminosilicate Catalysts. Brunauer Emmett Teller (BET) analysis of NiMo/ZSM-5, CoMo/HZSM-5, and Mo/HZSM-5 shown in Table 4, indicates that the aluminosilicate catalysts used in the upgrade of the bitumen showed high values for their surface area and pore volume, with average pore diameter in the mesopore range (2-50 nm) [15, 16]. Thus, each catalyst displayed a structure corresponding to a mesoporous aluminosilicate catalyst [17].

Summary of Optimised Agbabu Bitumen (Optimum Conditions). The numerical optimisation method involved setting a goal for each response to generate the optimal conditions while each factor selected was in default set goal – 'in range'. The optimisation goal was to minimise the viscosity, maximise the API gravity, minimise the residue yield and maximise the light oil yield as the responses. At the same time, the ranges of the factors (temperature, reaction time, and rice husks) are set as presented in Table 5.

Table 5 – Optimisation Criteria

Name	Goal	Lower Limit	Upper Limit
A: Temperature	is in range	300	350
B: Residence Time	is in range	30	180
C: Rice Husks	is in range	0.6	1
Viscosity	Minimise	20.63	68.924
API gravity	Maximise	19.99	24.52
Residue	Minimise	25.36	58.68
Light oil yield	Maximise	21.72	63.16

Table 5 shows the criteria used for the optimisation of Agbabu bitumen upgrading. While Table 6 shows some of the predicted optimisation results. The predicted responses under these conditions were 8.34 Pa.s, 24.52 °, 22.391 w/w% and 50.064 w/w% of viscosity, API gravity, residue yield and light oil yield.

Table 6 – Some of the Predicted Optimization Results

No	Temp. (°C)	Residence Time (min)	Rice Husks (%)	Viscosity (Pa.s)	API gravity (°)	Residue yield (w/w%)	Light oil yield (w/w%)	Desirability (Unity)	
1	345.716	30.000	1.000	8.340	24.520	22.391	50.064	0.909	Selected
2	345.935	30.007	1.000	8.160	24.559	22.407	49.870	0.908	
3	344.963	30.000	1.000	8.963	24.389	22.353	50.705	0.908	
4	345.825	30.703	1.000	8.611	24.520	22.487	49.844	0.908	
5	349.434	179.999	1.000	18.816	24.520	19.144	49.786	0.907	

Validation of the Optimum Conditions. The Agbabu bitumen upgrade was conducted at the optimum conditions (temperature of 345.716 °C, reaction time of 30.0 min and rice husks of 1.0 wt.%) to validate the result obtained from the Design Expert software. Table 7 compares the optimum value and validation value of the responses for the Agbabu bitumen upgrade after conduction at the optimum conditions.

Table 7 – Validation of the Optimum Conditions (Temp., 345.716 °C, Residence time of 30 Minutes and 1.0% of Rice husks)

No	Responses	Predicted value	Experimental Value	% Error
1	Viscosity	8.340	8.280	0.719
2	API gravity	24.520	24.351	0.689
3	Residue yield	22.390	22.56	0.759
4	Light oil yield	50.064	50.100	0.072

The result in Table 7 implied that variation between the optimum and validation value responses was minimal (this can be observed from the % error). Hence, this ascertains the accuracy of the results obtained from the optimisation.

Upgraded Agbabu Bitumen Analysis. The four experimental runs investigated in this work can be classified explicitly under thermal cracking (without catalyst) and catalytic thermal cracking (with catalyst). However, the parameter of interest is the effect of the three mesoporous catalysts (NiMo/ZSM-5, CoMo/HZSM-5 and Mo/HZSM-5) on the upgrading process at the optimum condition (temperature of 345.716 °C, residence time of 30.0 minutes and 1.0 wt.% of rice husks). The FT-IR and GC-MS analysis of each experimental run was conducted to ascertain the upgrade level by comparing and contrasting the heavy oil or bitumen before the upgrade and the upgraded oil after the upgrade or reaction. The results of employing the three mesoporous aluminosilicate catalysts were compared with the responses (viscosity, API gravity, residue and light oil yield) obtained at the optimum conditions (validation point/value) without catalysts, as shown in Table 8. Table 8 implies that bituminous oil was upgraded more when the catalyst was used. The performance of the upgrading process was measured through the following headings.

Viscosity, API gravity, and Light oil yield of optimised and upgraded Agbabu bitumen. The comparison of the viscosity, API gravity and light oil yield among the experimental runs with catalyst NiMo/ZSM-5 was observed to perform better in upgrading compared with catalysts CoMo/HZSM-5, Mo/HZSM-5 and optimal crude as shown in Table 8.

This can be attributed to the fact that the catalyst NiMo/ZSM-5 has more pore volume and surface area distribution than the other catalysts (CoMo/HZSM-5 and Mo/HZSM-5), thus more upgrade and yield. In addition, such catalysts are very effective in the catalytic transformations of bulk molecules of the bitumen due to the efficient transportation and diffusion of the reactants to the active sites and the reverse diffusion of the resulting reaction products [18].

Table 8 – Catalytic Optimised Agbabu Bitumen at Optimum Conditions

No	Experimental run	Responses			
		Viscosity (Pa.s)	API gravity (°)	Residue yield (w/w%)	Light oil yield (w/w%)
1	Optimal Crude	8.280	24.351	22.56	50.10
2	NiMo/ZSM-5 Catalyzed Crude	2.060	29.826	10.66	70.42
3	CoMo/HZSM-5 Catalyzed Crude	3.780	26.652	12.48	65.08
4	Mo/HZSM-5 Catalyzed Crude	3.160	27.984	12.12	68.66

From Table 8, the API gravity of the upgraded Agbabu bitumen falls within the range of medium crude oil (API gravity 22.3–31.1°) compared to conventional light crude oil of API gravity greater than 31.1° API. In some literature, medium crude oil is light crude oil with API gravity greater than 22° API [19].

Asphaltenes Reduction and Sulfur Removal. Saturates, Aromatics, Resins, and Asphaltenes (SARA) analysis is used to determine the organic components in crude oil based on the components above (SARA) according to their solubility and polarity. However, as an analytical technique, it is used to determine the quality of bitumen. Asphaltenes component is mainly responsible for the highly viscous nature of the bitumen. So, asphaltenes reduction is significant in determining the quality of bitumen in the oil industry. The decrease in asphaltenes in bitumen usually takes place through solvent deasphalting and bond cleavage to form lower molecular structures such as saturates, naphthenes, olefins, aromatics, and resins etc, through a general process known as organic cracking [2].

Desulphurisation is a significant reaction in upgrading heavy oil or bitumen. As a reaction, desulphurisation removes sulphur contained in the bitumen as heteroatoms. The less sulphur in the bitumen, the higher its price value in the global petroleum market. It is affirmed that dispersed mesoporous nano-catalyst has high tendencies of sulphur removal in desulphurisation reactions as the active sites of the catalyst can access and accommodate the bulky molecules of the bitumen [20, 21].

Table 9 shows the asphaltenes and sulfur reduction of Agbabu raw bitumen, optimal crude and catalytically upgraded Agbabu bitumen.

Table 9 – Asphaltenes Reduction and Sulfur Removal of Upgraded Agbabu Bitumen

No	Experimental Run	SARA (wt.%)			Sulfur (wt.%)	
		Saturates	Aromatics	Resins	Asphaltenes	Sulfur
1	Raw Bitumen	53.48	12.84	15.37	8.86	4.51
2	Optimal Crude	59.28	17.15	13.46	3.14	2.26
3	NiMo/ZSM-5 Catalyzed Crude	70.12	19.25	3.87	1.65	1.26
4	CoMo/HZSM-5 Catalyzed Crude	60.45	14.34	12.33	2.86	1.54
5	Mo/HZSM-5 Catalyzed Crude	67.53	16.41	4.85	2.10	1.89

NiMo/ZSM-5 catalysed crude has the lowest asphaltenes content of 1.65 wt.%, amounting to 81.38% reduction in asphaltenes; likewise, the sulfur content was observed to be 1.26 wt.%, amounting to 72.06% sulfur removal. The amount of sulfur it contains makes a particular crude sour or sweet. Sweet crude has deficient levels of sulfur, well under 1 wt.%, while sour oil has as much as 1-2 wt.% of sulfur [19]. Thus, all the Agbabu bitumen presented in Table 9 is sour crude.

H/C Ratio. The H/C ratio is one of the main characteristic properties used to measure the extent of upgrading. During hydrocracking, heavy molecules such as asphaltenes and resins are expected to break down into saturates and aromatics fragments, with some smaller molecules, partly associating with each other, increasing H/C ratio [22]. Table 10 shows that the H/C ratio of the raw Agbabu bitumen was 1.19:1, with an increment of 1.73:1, with catalyst NiMo/ZSM-5 as the highest H/C amongst the runs.

From an established work by [25] in which they employed Fe/ZSM-5, glycerol and biomass for the heavy oil upgrade, the upgraded oil has Carbon 65.22 wt.% and Hydrogen 9.13 wt.% which gave H/C ratio of 1.68:1.

Table 10 – Hydrogen to Carbon (H/C) Ratio of Upgraded Agbabu Bitumen

Experimental Run	Carbon (wt.%)	Hydrogen (wt.%)	Hydrogen/Carbon (H/C Ratio)
Raw Bitumen	76.64	7.67	1.19:1
Optimal Crude	73.53	7.58	1.23:1
NiMo/ZSM-5 Catalyzed Crude	87.7	12.71	1.73:1
CoMo/HZSM-5 Catalyzed Crude	67.32	7.11	1.26:1
Mo/HZSM-5 Catalyzed Crude	78.45	9.66	1.47:1

The initial raw heavy crude employed by [25] has Carbon 85.45 wt.% and Hydrogen 11.19 wt. %, which gave H/C ratio of 1.57:1 and, hence, an increase of H/C ratio from 1.57:1 to 1.68:1. Thus, by comparison, this shows the extent of achievement in this research work. The H/C ratio for the raw heavy crude (raw Agbabu bitumen) and upgraded NiMo/ZSM-5 catalysed crude oil at optimum conditions increases from 1.19:1 to 1.73:1, respectively.

FT-IR Analysis of Upgraded Agbabu bitumen. The FTIR spectrum of the Agbabu bitumen after the upgrade was used to analyse and identify variation in the functional group of the active components present (saturates, aromatics, resins, and asphaltenes) based on the peak value in the infrared radiation region.

1. FT-IR Analysis of Upgraded Agbabu Bitumen at Optimum Conditions. However, the spectra of the other four runs showed a visible remarkable change when compared to the spectrum of the raw Agbabu bitumen as there was chemical bond cleavage such that from the raw Agbabu bitumen spectrum (Figure 3) showing the peaks (3690.1 cm^{-1}, 3649.1 cm^{-1} and 3399.3 cm^{-1}) had all disappeared (the observable contour or bulge from the raw Agbabu bitumen spectrum) indicating that the asphaltenes content has decreased in the raw Agbabu bitumen thus converted to or broken down to lighter components like saturates, aromatics and in some cases resins [23]. Several peaks, such as 2370.6 cm^{-1}, 2050.0 cm^{-1}, 1889.8 cm^{-1}, 1699.7 cm^{-1}, 1453.7 cm^{-1}, 965.4 cm^{-1}, and 812.6 cm^{-1} absorption bands, appeared in Figure 8 that were not in Figure 3, which is an indication of bond cleavage to lower molecular fractions such as saturates and aromatics [24].

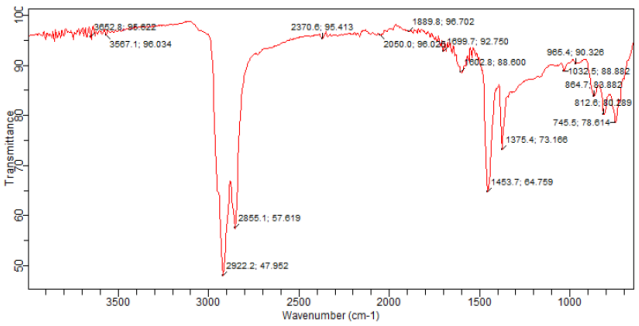

Figure 8 – FT-IR Spectrum of Upgraded Agbabu Bitumen at Optimum Conditions

The FT-IR spectrum of the upgraded Agbabu bitumen at optimum conditions, as shown in Figure 9, indicates that there were more observable peaks than the FT-IR of the raw Agbabu bitumen.

2. FT-IR Analysis of NiMo/ZSM-5 Catalyzed Upgraded Agbabu Bitumen. There are more observable peaks on the FT-IR of the upgraded Agbabu bitumen using NiMo/ZSM-5 at the optimum conditions when compared to the FT-IR of the raw Agbabu bitumen (Figure 9), indicating bond breakage from asphaltenes to resins and other lower oil components.

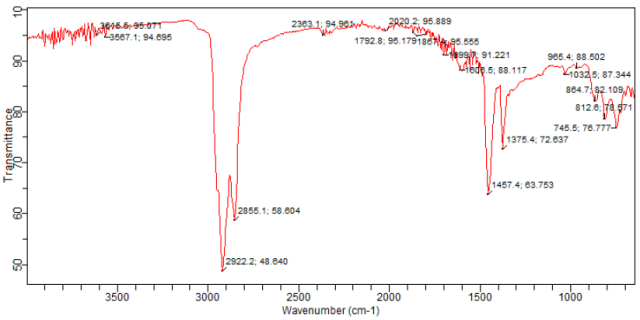

Figure 9 – FT-IR of NiMo/ZSM-5 Catalyzed Upgraded Agbabu Bitumen

Furthermore, the peaks 2363.1 cm^{-1}, 2020.2 cm^{-1}, 1867.4 cm^{-1}, 1792.8 cm^{-1}, 1699.7 cm^{-1}, and 1606.5 cm^{-1} absorption bands are primarily assigned to aliphatic saturated and unsaturated compounds, esters, and aromatics which is an indication of the bitumen upgrade [6].

3. FT-IR Analysis of CoMo/HZSM-5 Catalyzed Upgraded Agbabu Bitumen. There was not much upgrade on the Agbabu bitumen using CoMo/HZSM-5 catalyst as the peaks shown in the FT-IR spectrum in Figure 10 indicate lesser peaks compared to the FTIR spectrum obtained for the upgraded Agbabu bitumen at the optimum conditions and that of the catalysed NiMo/ZSM-5 upgraded Agbabu bitumen.

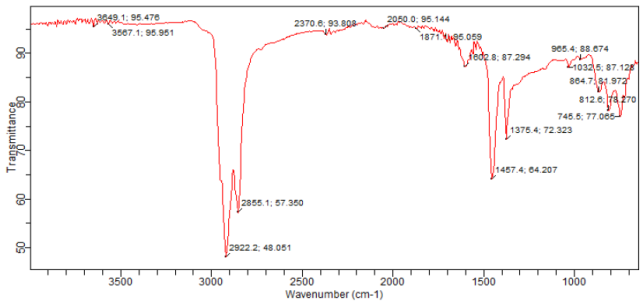

Figure 10 – FT-IR of CoMo/HZSM-5 Catalyzed Upgraded Agbabu Bitumen

Thus, there is lesser conversion to lower compounds of the functional group. The only differences in the peaks are 2050.0 cm^{-1}, 1871.1 cm^{-1}, and 1602.8 cm^{-1} absorption bands, which are assigned to (aromatic combination bands, transition metal carbonyls), five-membered ring aldehyde and (alkenyl C=C stretch, conjugated C=C) respectively [9].

4. FT-IR Analysis of Mo/ZSM-5 Catalyzed Upgraded Agbabu Bitumen. There were visible absorption bands shown in Figure 11, and most of the bond cleavage ends in the aromatics group.

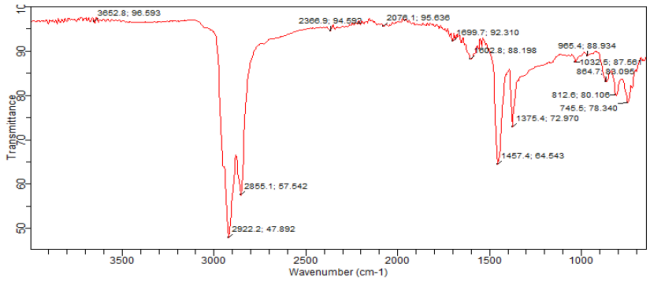

Figure 11 – FT-IR of Mo/HZSM-5 Catalyzed Upgraded Agbabu Bitumen

The visible absorption bands in Figure 11, different from all the FTIR discussed earlier, are 2366.9 cm^{-1}, 2076.1 cm^{-1}, and 1699.7 cm^{-1} absorption bands, and are assigned to (C≡C group, NH component), Isothiocyanate (-NCS), and C=O in aromatic carboxylic acids), respectively [6]. Amongst the three catalysts employed (NiMo/ZSM-5, CoMo/HZSM-5, and Mo/HZSM-5) in carrying out the Agbabu bitumen upgrade, catalyst Mo/HZSM-5 has the minor conversion to lower molecules as most of its' aromatics not converted to lower compounds but rather the asphaltenes were converted to more aromatics resulting to more aromatics peaks on the FT-IR spectrum [8]. This effect of Mo/HZSM-5 catalyst on the Agbabu bitumen upgrade can be much felt or understood from the GC-MS spectrum of the upgraded Agbabu bitumen using Mo/HZSM-5 at optimum conditions.

A cascaded graph of the FT-IR spectrum of the raw Agbabu bitumen, optimal crude, NiMo/ZSM-5 catalysed crude, CoMo/HZSM-5 catalysed crude and Mo/HZSM-5 catalysed crude run are displayed on a single graph shown in Figure 12 for contrast and comparison. The spectra of the other four runs showed a visible remarkable change when compared to the spectrum of the raw Agbabu bitumen, as there was chemical composition shift/bond cleavage such that the asphaltenes region from the raw bitumen spectrum showing the peak (3849.1 cm^{-1}, 94.336%) and (3399.3 cm^{-1}, 89.675%) have all disappeared (the observable contour or bulge from the raw bitumen spectrum) indicating that the asphaltenes content has decreased in the raw Agbabu bitumen thus converted to or broken down to lighter components like saturates, aromatics and in some cases resins.

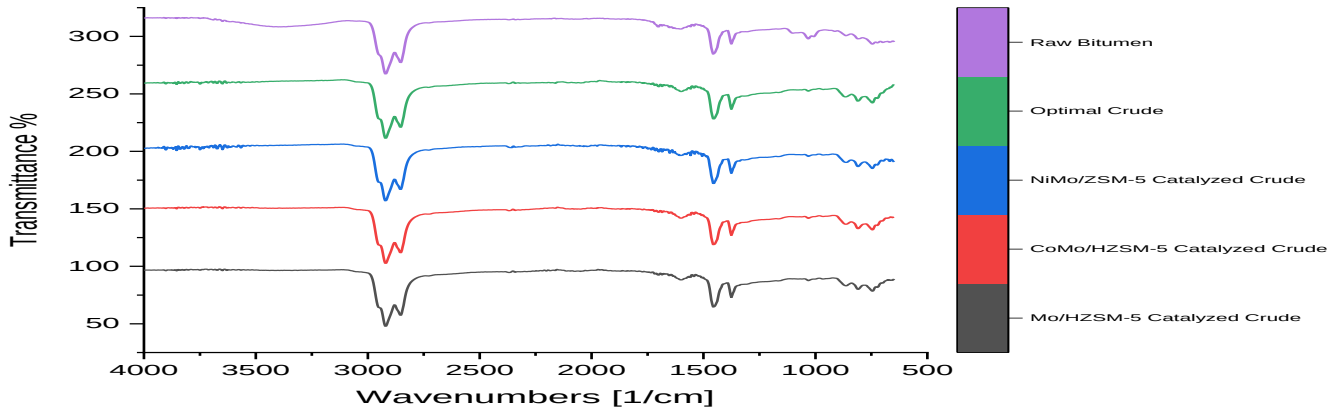

Figure 12 – FT-IR Spectrum of the Raw Agbabu Bitumen Before and After Upgrade

GC-MS Analysis of Agbabu Bitumen. The results of the GC-MS analysis led to the identification of several compounds from the GC fractions of the raw bitumen after the upgrade. These compounds were identified through mass spectrometry attached to the GC.

1. GC-MS Analysis of Optimised Agbabu Bitumen. From GC-MS analysis of the run "optimal crude" without catalyst – (Raw bitumen + 1.0 wt.% Rice husks @ 345.716 °C, 30 min), 21 different compounds were identified as shown in Table 11 and Figure 13 shows the GC-MS spectrum for the run "optimal crude" without catalyst.

2. GC-MS Analysis of NiMo/ZSM-5 Catalyzed Agbabu Bitumen. From GC-MS analysis of the run "NiMo/ZSM-5 catalysed crude", 73 different compounds were identified, as shown in Table 12, and Figure 14 shows the GC-MS spectrum of NiMo/ZSM-5 catalysed Agbabu bitumen. The NiMo/ZSM-5 catalysed Agbabu bitumen has more chemical compounds than the GC-MS spectrum of the raw Agbabu bitumen, with only 42 chemical compounds identified. This indicates an upgrade from higher molecular fractions to lower molecular fractions.

3. GC-MS Analysis of CoMo/HZSM-5 Catalyzed Agbabu Bitumen. From GC-MS analysis of the run "CoMo/HZSM-5 catalysed crude", ten different compounds were identified, as shown in Table 13, and Figure 15 shows the GC-MS spectrum of CoMo/HZSM-5 catalysed Agbabu bitumen. From the spectrum, the CoMo/HZSM-5 catalyst does not favour the bitumen upgrade, as most of the asphaltene components were only broken down to resins rather than aromatics and saturates.

4. GC-MS Analysis of Mo/HZSM-5 Catalyzed Agbabu Bitumen. From GC-MS analysis of the run "Mo/HZSM-5 catalysed crude," 61 different compounds were identified, as shown in Table 14. Figure 16 shows the GC-MS spectrum of Mo/HZSM-5 catalysed Agbabu heavy crude oil. There was also a noticeable upgrade of the Agbabu bitumen with the Mo/HZSM-5 catalysed reaction, as the asphaltenes bond cleavage mostly ends to form aromatic compounds, a few resins, and saturates.

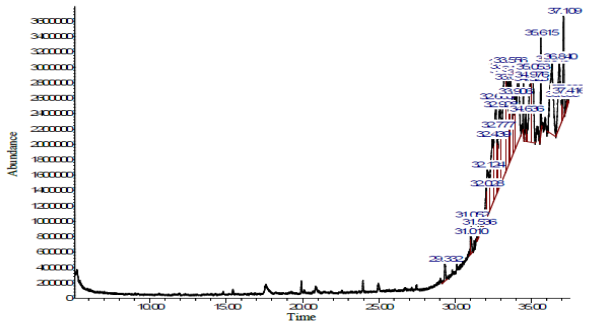

Figure 13 – GC-MS Spectra of Optimised Agbabu Bitumen

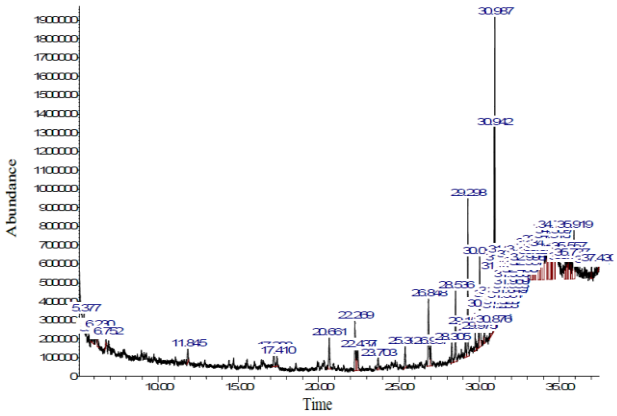

Figure 14 – GC-MS Spectrum of NiMo/ZSM-5 Catalyzed Agbabu Bitumen

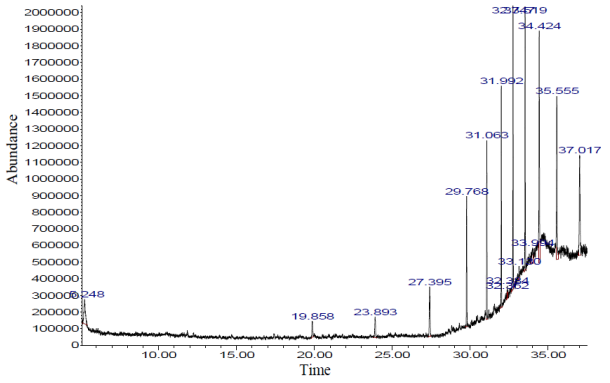

Figure 15 – GC-MS Spectrum of CoMo/HZSM-5 Catalyzed Agbabu Bitumen

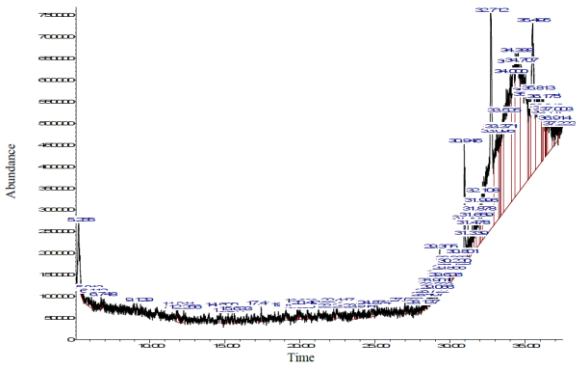

Figure 16 – GC-MS Spectrum of Mo/HZSM-5 Catalyzed Agbabu Bitumen

Table 11 – Chemical Composition of Optimised Agbabu Bitumen from GC-MS Analysis

No	Chemical Compound	CAS No	Mol. Formula	Mol. Wt. (g/mol)	Nature of Compounds
1	Z,Z-6,24-Tritriacontadien-2-one	1000111-38-8	$C_{33}H_{64}O$	476.90	-
2	trans-2-Ethyl-2-hexen-1-ol	1000139-52-3	$C_8H_{16}O$	128.21	-
3	Pentatriacontane, 13-docosenylidene-	1000156-09-1	$C_{47}H_{94}$	659.20	-
4	Pentadecanoic acid, 13-methyl-, methyl ester	005487-50-3	$C_{17}H_{34}O_2$	270.45	Aromatic
5	n-Tridecan-1-ol	000112-70-9	$C_{13}H_{28}O$	200.36	-
6	Lup-20(29)-en-3-ol, acetate, (3.beta.)-	001617-68-1	$C_{32}H_{52}O_2$	468.75	-
7	Hexadecanoic acid, 2-hydroxy-, methyl ester	016742-51-1	$C_{17}H_{34}O_3$	286.40	Aromatic
8	Cyclotriacontane	000297-35-8	$C_{30}H_{60}$	420.80	Saturate
9	Cyclononasiloxane, octadecamethyl-	000556-71-8	$C_{18}H_{54}O_9Si_9$	667.40	Resin
10	Cyclohexane, (1-hexadecylheptadecyl)-	055517-75-4	$C_{39}H_{78}$	547.04	Saturate
11	Carbamic acid, N-(4-chlorophenyl)-, 4-nitrophenyl ester	003848-41-7	-	-	Aromatic
12	Borane, 2,3-dimethyl-2-butyl- (dimer)	1000159-64-3	$C_{12}H_{30}B_2$	196.00	-
13	benzenesulfonyl fluoride, 4-(hexadecyloxy)-3-nitro-	1000402-84-4	$C_{22}H_{36}FNO_5S$	445.60	Aromatic
14	9,19-Cyclolanostan-3-ol, 24,24-epoxymethano-, acetate	1000190-57-2	$C_{33}H_{54}O_3$	498.80	Resin
15	7,10-Octadecadienoic acid, methyl ester	056554-24-6	$C_{19}H_{34}O_2$	294.47	Aromatic
16	4-Trifluoroacetoxytetradecane	1000245-47-6	$C_{16}H_{29}F_3O_2$	310.39	-
17	1-Heptadecanamine	004200-95-7	$C_{17}H_{37}N$	255.48	-
18	1,3,5,7,9,11-Hexavinyl-3,5,9,11-tetrabutoxybicyclo[5.5.1]hexasiloxane	110991-14-5	-	-	Resin
19	1,22-Docosanediol	022513-81-1	-	-	-
20	1,1,1,5,7,7,7-Heptamethyl-3,3 bis(trimethylsiloxy)tetrasiloxane	038147-00-1	$C_{13}H_{39}O_5Si_6$	443.96	Resin
21	.alpha.-d-Glucose, 4,6-O-isopropylidene-1-O-methyl-6-O-[4-bromobenzenesulfonate]	1000127-18-3	$C_{22}H_{36}BrO_8S$	453.30	Aromatic

Table 12 – Chemical Composition of NiMo/ZSM-5 Catalyzed Agbabu Bitumen from GC-MS Analysis

No	Chemical Compound	CAS No	Mol. Formula	Mol. Wt. (g/mol)	Nature of Compounds
1	Z-8-Hexadecene	1000130-87-5	$C_{16}H_{32}$	224.43	-
2	trans-13-Octadecenoic acid	000693-71-0	$C_{18}H_{34}O_2$	282.46	-
3	17-hexadecyltetratriacontane	055256-07-0	$C_{50}H_{102}$	703.34	Saturate
4	Phthalic acid, pentyl 2,4,6-trichlorobenzyl ester	1000382-87-9	-	-	Aromatic
5	Phenanthrene-10-ethanamine, 3-bromo-.beta.-hydroxy-N,N-diheptyl-, hydrosulfate	049647-04-3	-	-	-
6	Pentadecanoic acid, 13-methyl-, methyl ester	005487-50-3	$C_{17}H_{34}O_2$	270.45	Aromatic
7	13-Undecylpentacosane	055517-89-0	$C_{47}H_{74}$	506.58	Saturate
8	Pennogenin diacetate	065380-31-6	$C_{31}H_{46}O_6$	514.7	-
9	Palmitoleic acid	000373-49-9	$C_{16}H_{30}O_2$	254.41	-
10	Ttetradecyloxirane	007320-37-8	$C_{16}H_{32}O$	240.43	Resin
11	Oleic Acid	000112-80-1	$C_{18}H_{34}O_2$	282.46	-
12	Nickel, bis[bis(2-methylpropyl) carbamodithioato-S,S']-, (SP-4-1)-	015317-78-9	$C_{18}H_{36}N_2NiS_4$	467.45	Resin
13	Methyl 8-methyl-decanoate	1000336-49-1	$C_{12}H_{24}O_2$	200.32	Aromatic
14	Methyl 2-hydroxy-pentacosanoate	118745-42-9	$C_{26}H_{52}O_3$	412.70	Aromatic
15	Hexadecanoic acid, methyl ester	000112-39-0	$C_{17}H_{34}O_2$	270.50	Aromatic
16	Hexadecanenitrile	000629-79-8	$C_{16}H_{31}N$	237.42	-
17	Hexadecane	000544-76-3	$C_{16}H_{34}$	226.44	Saturate
18	Heptylcyclohexane	005617-41-4	$C_{13}H_{26}$	182.35	Saturate
19	Heptadecanoic acid, 16-methyl-, methyl ester	005129-61-3	$C_{19}H_{38}O_2$	298.50	Aromatic

No	Chemical Compound	CAS No	Mol. Formula	Mol. Wt. (g/mol)	Nature of Compounds
20	Estra-1,3,5(10)-trien-17.beta.-ol	002529-64-8	$C_{18}H_{24}O$	256.39	Aromatic
21	E-14-Hexadecenal	330207-53-9	$C_{16}H_{30}O$	238.41	-
22	E-11-Hexadecenal	1000130-86-1	$C_{16}H_{30}O$	238.41	-
23	Dodecanoic acid, methyl ester	000111-82-0	$C_{13}H_{26}O_2$	214.34	Aromatic
24	Diethyl Phthalate	000084-66-2	$C_{12}H_{14}O_4$	222.40	Aromatic
25	Decanoic acid, ethyl ester	000110-38-3	$C_{12}H_{24}O_2$	200.32	Aromatic
26	Cyclohexanol, 2-(2-propynyloxy)-, trans-	007229-32-5	$C_9H_{14}O_2$	154.21	-
27	Undecylcyclohexane	054105-66-7	$C_{17}H_{34}$	238.45	Saturate
28	Cyclohexane, 1,1'-(1-methyl-1,3-propanediyl)bis-	041851-35-8	$C_{16}H_{30}$	222.41	Saturate
29	cis-9-Hexadecenal	056219-04-6	$C_{16}H_{30}O$	238.41	Aromatic
30	cis-13-Octadecenoic acid, methyl ester	1000333-58-3	$C_{19}H_{36}O_2$	296.50	Aromatic
31	cis-11-Hexadecenal	053939-28-9	$C_{16}H_{30}O$	238.41	Aromatic
32	Bicyclo[10.8.0]eicosane, (E)-	1000155-85-0	$C_{20}H_{38}$	275.50	Saturate
33	Benzene, 1,2,3-trifluoro-4-nitro-	000771-69-7	$C_6H_2F_3NO_2$	177.08	Aromatic
34	Allopregan-3,16-diol, O,O'-diacetyl-20-s-[3-methylpyrid-6-yl]-	1000214-17-9	-	-	-
35	Acetyl chloride, chloro-	000079-04-9	$C_2H_2Cl_2O$	112.94	-
36	9-Tetradecenal, (Z)-	053939-27-8	$C_{14}H_{26}O$	210.36	-
37	9-Octadecenoic acid, methyl ester, (E)-	001937-62-8	$C_{19}H_{36}O_2$	296.50	Aromatic
38	9-Octadecenoic acid, (E)-	000112-79-8	$C_{18}H_{34}O_2$	282.50	-
39	9-Octadecenoic acid (Z)-, 2,3-dihydroxypropyl ester	000111-03-5	$C_{21}H_{40}O_4$	356.50	Aromatic
40	9-Octadecenal	005090-41-5	$C_{18}H_{34}O_2$	266.5	-
41	9-Nonadecene	031035-07-1	$C_{19}H_{38}$	266.51	-
42	9-Heptadecanone	000540-08-9	$C_{17}H_{34}O$	254.50	-
43	9,19-Cyclolanostan-3-ol, 24,24-epoxymethano-, acetate	1000190-57-2	$C_{33}H_{54}O_3$	498.80	Resin
44	8-Cyclohexadecen-1-one	003100-36-5	$C_{16}H_{28}O$	236.39	-
45	8,11-Octadecadienoic acid, methyl ester	056599-58-7	$C_{19}H_{34}O_2$	294.26	Aromatic
46	7-Oxabicyclo[4.1.0]heptane, 1,5-dimethyl-	162239-52-3	$C_8H_{14}O$	126.20	-
47	7-Hexadecene, (Z)-	035507-09-6	$C_{16}H_{32}$	224.42	-
48	5-Octadecene, (E)-	007206-21-5	$C_{18}H_{36}$	252.48	-
49	4-Trifluoroacetoxypentadecane	1000245-47-9	$C_{17}H_{31}F_3O_2$	324.40	-
50	4-n-Hexylthiane, S,S-dioxide	070928-52-8	$C_{11}H_{22}O_2S$	218.36	-
51	4-Hydroxyphenyllactic acid, 3TBDMS derivative	1000221-80-2	$C_{27}H_{52}O_4Si_3$	524.96	Resin
52	4-Androsten-4-chloro-3.alpha.-ol-17-one, di-trimethylsilyl	1000412-24-8	$C_{26}H_{43}ClO_2Si_2$	479.20	Resin
53	4-(Diethylphosphoryl)-4-methylpentan-2-one	015090-36-5	$C_{10}H_{21}O_2P$	204.25	-
54	3-Nonenoic acid, ethyl ester	091213-30-8	$C_{11}H_{20}O_2$	184.28	Aromatic
55	3'H-Cycloprop(1,2)-5-cholest-1-en-3-one, 1'-carboethoxy-1'-cyano-1,2-dihydro-	075857-80-6	$C_{32}H_{49}NO_3$	495.37	Resin
56	3-Aza-2-oxabicyclo[2.2.2]oct-5-ene, 3-acetyl-7-endo,8-exo-dimethoxy-	102724-50-5	-	-	-
57	2-Methyl-Z,Z-3,13-octadecadienol	1000130-90-5	$C_{19}H_{36}O$	280.50	-
58	2-Hexyldecyl isobutyrate	1000368-55-3	$C_{20}H_{40}O_2$	312.50	-
59	2-Dodecen-1-yl(-)succinic anhydride	019780-11-1	$C_{16}H_{26}O_3$	266.38	Aromatic
60	2,5-Furandione, 3-dodecyl-	059426-46-9	$C_{16}H_{26}O_3$	266.38	Aromatic
61	2,3-Di[p-chlorophenyl]-5,8-dimethoxy-6-acetamidoquinoxaline	056393-33-0	-	-	-
62	1-Hexadecanol	036653-82-4	$C_{16}H_{34}O$	242.44	-
63	1-Eicosene	003452-07-1	$C_{20}H_{40}$	280.53	-
64	1-Decyloxy-2-nitrobenzene	098311-79-6	$C_{16}H_{25}NO_3$	279.38	Aromatic
65	13-Octadecenoic acid, methyl ester	056554-47-3	$C_{19}H_{36}O_2$	296.50	Aromatic

No	Chemical Compound	CAS No	Mol. Formula	Mol. Wt. (g/mol)	Nature of Compounds
66	12-Methyl-E,E-2,13-octadecadien-1-ol	1000130-90-4	$C_{19}H_{36}O$	280.50	-
67	11-Dodecen-1-ol trifluoroacetate	128792-46-1	$C_{14}H_{23}F_3O_2$	280.33	-
68	1-[3,3-Difluoro-1-(pentafluoroethyl)-2-(trifluoromethyl)prop-2-en-1-ylidene]-2-[2,2,2-trifluoro-1-(trifluoromethyl)ethylidene]hydrazine	1000394-35-5	-	-	-
69	1,3-Dimethyl-4,8-dioxatricyclo[5.1.0.0(3,5)]octane-2,6-diol	1000186-19-0	-	-	-
70	1,3,5,7,9,11-Hexavinyl-3,5,9,11-tetrabutoxybicyclo[5.5.1]hexasiloxane	110991-14-5	-	-	-
71	1-(3-Acetamidophenyl)-3-(2,2,2-trichloro-1-isovaleramidoethyl)-2-thiourea	294658-29-0	-	-	-
72	[2-Acetyl-3-(2,4-dichlorophenyl)-5-(2,4-dichlorostyryl)-3,4-dihydrophenoxy]difluoroborane	1000223-62-4	-	-	-
73	(S)-(+)-Epichlorohydrin	067843-74-7	C_3H_5ClO	92.52	Resin

Table 13 – Chemical Composition of CoMo/HZSM-5 Catalyzed Agbabu Bitumen from GC-MS Analysis

No	Chemical Compound	CAS No	Mol. Formula	Mol. Wt. (g/mol)	Nature of Compounds
1	Pyridine-3-carboxamide, oxime, N-(2-rifluoromethylphenyl)-	288246-53-7	$C_{13}H_{10}F_3N_3O$	281.23	-
2	Morphine, 2TMS derivative	055449-66-6	$C_{23}H_{35}NO_3Si_2$	429.70	Resin
3	Hexasiloxane, tetradecamethyl-	000107-52-8	$C_{14}H_{42}O_5Si_6$	458.99	Resin
4	Dodecyl propyl ether	1000406-27-7	$C_{15}H_{32}O$	228.41	Aromatic
5	Dihydrophytol, TMS derivative	078695-20-2	$C_{23}H_{50}OSi$	370.70	-
6	Cyclononasiloxane, octadecamethyl-	000556-71-8	$C_{18}H_{54}O_9Si_9$	667.36	Resin
7	3-Isopropoxy-1,1,1,7,7,7-hexamethyl-3,5,5-tris(trimethylsiloxy)tetrasiloxane	071579-69-6	$C_{18}H_{52}O_7Si_7$	577.2	Resin
8	3'H-Cycloprop(1,2)-5-cholest-1-en-3-one, 1'-carboethoxy-1'-cyano-1,2-dihydro-	075857-80-6	$C_{32}H_{49}NO_3$	495.70	Resin
9	3-Bromo-N-(3,5-dichlorophenyl)benzamide, TMS derivative	1000331-99-9	$C_{16}H_{16}Br_2Cl_2NOSi$	417.2	Resin
10	1,1,1,5,7,7,7-Heptamethyl-3,3 bis(trimethylsiloxy)tetrasiloxane	038147-00-1	$C_{13}H_{40}O_5Si_6$	444.97	Resin

Table 14 – Chemical Composition of Mo/HZSM-5 Catalyzed Agbabu Heavy Bitumen from GC-MS Analysis

No	Chemical Compound	CAS No	Mol. Formula	Mol. Wt. (g/mol)	Nature of Compounds
1	Z-6,17-Octadecadien-1-ol acetate	086252-73-5	$C_{20}H_{36}O_2$	308.50	-
2	Z,E-2-Methyl-3,13-octadecadien-1-ol	1000131-10-5	$C_{19}H_{36}O$	280.50	-
3	Undec-10-ynoic acid, tridec-2-yn-1-yl ester	1000406-96-9	$C_{24}H_{40}O_2$	360.60	Aromatic
4	Trimyristin	000555-45-3	$C_{45}H_{86}O_6$	723.16	Aromatic
5	trans-2-Hexenoic acid, 5-methyl-2-isopropyl-, methyl ester	1000139-87-5	$C_{11}H_{20}O_2$	184.27	Aromatic
6	Thiourea, 2-cyano-1,3-dihexyl-	056342-27-9	$C_{14}H_{26}N_2S_2$	286.50	-
7	Tetracosanoic acid, heptyl ester	1000405-21-9	$C_{20}H_{40}O_2$	312.50	Aromatic
8	Sulfurous acid, 2-propyl undecyl ester	1000309-12-2	$C_{14}H_{30}O_3S_2$	278.45	Aromatic
9	Succinic acid, 4-chloro-3-methylphenyl tetrahydrofurfuryl ester	1000390-72-4	-	-	-
10	Spiro[2,4,5,6,7,7a-hexahydro-2-oxo-4,4,7a-trimethylbenzofuran]-7,2'-(oxirane)	1000197-10-9	$C_{12}H_6O_3$	208.25	Aromatic
11	Sclareolide	000564-20-5	$C_{16}H_{26}O_2$	250.38	Aromatic

No	Chemical Compound	CAS No	Mol. Formula	Mol. Wt. (g/mol)	Nature of Compounds
12	1-(2-furanylcarbonyl)piperazine	040172-95-0	$C_9H_{12}N_2O_2$	180.20	Aromatic
13	Phenanthrene-10-ethanamine, 3-bromo-.beta.-hydroxy-N,N-diheptyl-, hydrosulfate	049647-04-3	$C_{30}H_{42}BrNO_4S$	592.63	Aromatic
14	Oxirane, tetradecyl-	007320-37-8	$C_{16}H_{32}O$	240.42	Resin
15	2-methyloctane	003221-61-2	C_9H_{20}	128.26	Saturate
16	N-Pyrrylcarbinol	092776-61-9	C_5H_7NO	97.12	-
17	N-Benzyl-N-ethyl-p-isopropylbenzamide	015089-22-2	$C_{19}H_{23}NO$	281.40	Aromatic
18	N-(3-Amino-1,4-dioxo-1,4-dihydronaphthalen-2-yl)-N-phenylacetamide	004497-84-1	$C_{18}H_{14}N_2O_3$	306.30	Aromatic
19	Muscimol	002763-96-4	$C_4H_6N_2O_2$	114.10	-
20	Isopulegol	000089-79-2	$C_{10}H_{18}O$	154.25	Aromatic
21	Tetradecamethylhexasiloxane	000107-52-8	$C_{14}H_{42}O_5Si_6$	458.99	Resin
22	Hexadecanoic acid, methyl ester	000112-39-0	$C_{17}H_{34}O_2$	270.50	Aromatic
23	Eicosyl isobutyl ether	1000406-33-0	$C_{23}H_{48}O$	340.60	-
24	E-8-Methyl-9-tetradecen-1-ol acetate	1000130-81-4	$C_{17}H_{32}O_2$	268.40	-
25	E-10-Octadecen-1-ol acetate	002195-92-8	$C_{20}H_{38}O_2$	310.50	-
26	Diethyl[[3-octylsulfonyl]-4-n-butylanilinomethylene]malonate	1000214-51-0	-	-	-
27	Decyl heptyl ether	1000406-39-1	$C_{17}H_{36}O$	256.50	Aromatic
28	Cyclopropane, 1-chloro-1-ethyl-2,2,3-trimethyl-	061142-56-1	$C_8H_{15}Cl$	146.66	-
29	1,2,4,5-tetraethylcyclohexane	061142-00-5	$C_{14}H_{28}$	196.37	Saturate
30	1-aminomethylcyclododecanol	000832-29-1	$C_{13}H_{27}NO$	213.36	-
31	Cyclodisilazane-2,2,4,4-tetramine, N,N,N',N'-tetramethyl-1,3-bis[tris(methylamino)silyl]-	034665-55-9	$C_{10}H_{40}N_{12}Si_4$	440.84	Resin
32	Borane, isopropyldipropyl-	010325-43-6	$C_9H_{21}B$	140.07	-
33	Bicyclo[2.2.1]heptane-1-carboxylic acid, 7,7-dimethyl-2-oxo-, (3,4-difluorophenyl)amide	1000315-99-0	-	-	-
34	Bicyclo[2.2.1]heptane-1-carboxylic acid, 4,7,7-trimethyl-3-oxo-2-oxa-, (4-trifluoromethylphenyl)amide	1000315-86-8	-	-	-
35	9-Undecenal, 2,6,10-trimethyl-	000141-13-9	$C_{14}H_{26}O$	210.36	-
36	9-Tetradecen-1-ol, (E)-	052957-16-1	$C_{14}H_{28}O$	212.37	-
37	9,12-Octadecadienoic acid, methyl ester, (E,E)-	002566-97-4	$C_{19}H_{34}O_2$	294.50	Aromatic
38	8-Heptadecene	002579-04-6	$C_{17}H_{34}$	238.50	-
39	8,8,9-Trimethyl-deca-3,5-diene-2,7-dione	1000194-25-9	$C_{13}H_{20}O_2$	208.30	-
40	6-Bromohexanoic acid, 2-bromo-4-fluorophenyl ester	1000293-66-9	$C_9H_{13}Br_2FO_2$		Aromatic
41	6-Amino-1,3,5-triazine-2,4(1H,3H)-dione	000645-93-2	$C_3H_4N_4O_2$	128.09	-
42	5-Hydroxy-1-(4-methoxy-phenyl)-5-phenyl-pyrrolidine-2,3-dione	1000296-82-7	$C_{17}H_{15}NO_4$	297.31	Aromatic
43	4-Methyl-trans-3-thiabicyclo[4.4.0]decane	1000215-94-1	-	-	-
44	3H-Cyclodeca[b]furan-2-one, 4,9-dihydroxy-6-methyl-3,10-dimethylene-3a,4,7,8,9,10,11,11a-octahydro-	1000310-90-7	$C_{15}H_{20}O_4$	264.32	Aromatic
45	3,5-Dimethyl-4-chloroisoxazole	010557-86-5	C_5H_6ClNO	131.56	Aromatic
46	3,4-Diiodo-3,4-dedioxy-1,2:5,6-diacetone dulcitol	1000129-83-6	-	-	-
47	2-Pentadecanone, 6,10,14-trimethyl-	000502-69-2	$C_{18}H_{36}O$	268.48	-
48	2-Methyl-Z,Z-3,13-octadecadienol	1000130-90-5	$C_{19}H_{36}O$	280.50	-
49	2H-Inden-2-one, octahydro-3a-methyl-, trans-	020379-99-1	$C_{10}H_{16}O$	152.23	Aromatic

No	Chemical Compound	CAS No	Mol. Formula	Mol. Wt. (g/mol)	Nature of Compounds
50	2H-Bisoxireno[2,3:8,8a]azuleno[4,5-b]furan-7(3aH)-one, octahydro-3a,8c-dimethyl-6-methylene-, (1aR,2aR,3aS,5aS,8aS,8bS,8cS)-	139343-89-8	$C_{15}H_{18}O_4$	262.12	Resin
51	2,5-Dihydroxybenzoic acid, 3TMS derivative	003618-20-0	$C_{16}H_{30}O_4Si_3$	370.66	Resin
52	2,4-Hexadienoic acid, ethyl ester, (2E,4E)-	002396-84-1	$C_8H_{12}O_2$	140.18	Aromatic
53	1-methyl-4-(prop-1-en-2-yl)-7-oxabicyclo[4.1.0]heptan-2one	1000365-66-7	-	-	-
54	1H-Indene, 2-butyl-5-hexyloctahydro-	055044-33-2	$C_{19}H_{36}$	264.50	Saturate
55	1H-Inden-1-one, 2,3-dihydro-3,3,5,6-tetramethyl-	054789-22-9	$C_{13}H_{16}O$	188.27	Aromatic
56	1-Ethyl-3,trans-(1,1-dimethylethyl)-4,trans-methoxycyclohexan-1-ol	1000215-62-5	$C_{13}H_{26}O_2$	214.34	-
57	1-Chloroeicosane	042217-02-7	$C_{20}H_{41}Cl$	316.99	
58	17-(1,5-Dimethylhexyl)-10,13-dimethyl-4-vinylhexadecahydrocyclopenta[a]phenanthren-3-ol	1000210-86-9	$C_{29}H_{50}O$	414.70	Resin
59	1,3,5,7,9,11-Hexavinyl-3,5,9,11-tetrabutoxybicyclo[5.5.1]hexasiloxane	110991-14-5	-	-	Resin
60	[1,2,4]Triazolo[1,5-a]pyrimidine, 2-butylsulfanyl-5,7-dimethyl-	1000304-65-4	-	-	-
61	[1,2,3,4]Tetrazolo[1,5-a]pyridin-8-amine	073721-28-5	$C_5H_5N_5$	135.13	Aromatic

Produced Gases from Upgraded Agbabu Bitumen. The composition of gases produced during the catalytic upgrading process was analysed using a natural gasboard gas analyser (Gasboard 3100P) to determine the volume percentage of CH_4 and H_2. Table 15 shows the volume percentage of the gases produced in each experimental run. From an overview of all the experimental runs, as shown in Table 15, methane (CH_4) gas represents the highest volume percentage of gas produced compared to H_2. The NiMo/ZSM-5 catalysed reaction produced the highest volume percentage of 54.82% CH_4 gas and 7.24% H_2 gas.

Table 15 – Volume Percentage of Gases Produced from Upgraded Agbabu Bitumen

No	Experimental run	Produced gases (vol.%)	
		CH_4	H_2
1	Optimal crude	39.93	5.71
2	NiMo/ZSM-5 catalyzed crude	54.82	7.24
3	CoMo/HZSM-5 catalyzed crude	45.46	5.05
4	Mo/HZSM-5 catalyzed crude	51.23	6.41

It is expected to have no CO and CO_2 as the reaction occurs without oxygen because the reactor was airtight and took place in an inert medium (N_2 medium). Thus, the rate of the oxidation process was limited due to the absence of oxygen [25].

The Extent of Upgrade of Upgraded Agbabu Bitumen. The extent of upgrading of the Agbabu bitumen was calculated or carried out to know the degree to which the Agbabu bitumen was upgraded. The parameters used were viscosity, API gravity, asphaltenes, sulfur, and H/C. Table 16 shows the properties of raw, optimal and catalysed upgraded Agbabu bitumen.

From all the upgrades carried out with and without catalyst at the optimum conditions, NiMo/ZSM-5 catalysed crude exhibits highest percentage upgrade in all the parameters with 97.63% viscosity reduction, 278.98% API gravity increase, 81.38% asphaltenes reduction, 72.06% sulfur removal, 45.38% H/C ratio increase as presented in Figure 17 which shows the summary in bar chart representation of the extent of upgrade of the upgraded Agbabu bitumen.

Table 16 – Properties of Raw, Optimal and Catalyzed Upgraded Agbabu Bitumen

Raw Bitumen / Upgraded Oil	Parameter				
	Viscosity (Pa.s)	API Gravity (°)	Asphaltenes (wt.%)	Sulfur (wt.%)	H/C
Raw bitumen	86.780	7.870	8.86	4.51	1.19
Optimal crude	8.280	24.351	3.14	2.26	1.23
NiMo/ZSM-5 catalyzed crude	2.060	29.826	1.65	1.26	1.73
CoMo/HZSM-5 catalyzed crude	3.780	26.652	2.86	1.54	1.26
Mo/HZSM-5 catalyzed crude	3.160	27.894	2.10	1.89	1.47

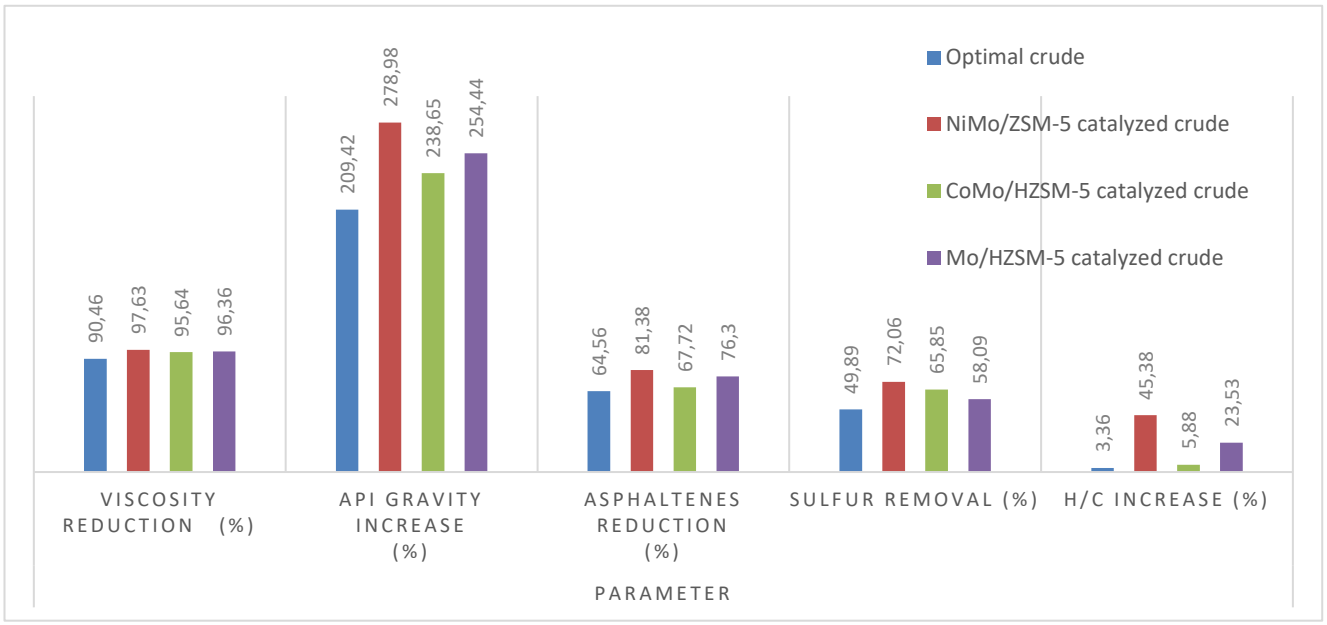

Figure 17 – Extent of Upgrade of Upgraded Agbabu Bitumen

CONCLUSIONS

Three mesoporous catalysts (NiMo/ZSM-5, CoMo/HZSM-5, and Mo/HZSM-5) were used to test and thus further upgrade Nigeria Agbabu bitumen in an autoclave batch reactor operating at optimum conditions (Temp., 345.716 °C, Residence time 30 min and 1.0 wt.% Rice husks) and a pressure of 32 bar nitrogen to investigate the effect of the three mesoporous aluminosilicate catalysts in the presence of rice husks on the Agbabu bitumen upgrade. This effect was studied with the viscosity reduction, API gravity increase, micro-carbon residue, light oil yield, asphaltenes reduction, sulphur removal/reduction, SARA wt.%, produced gas, and H/C ratio increase. The Agbabau bitumen before upgrade and after the upgrade was characterised for FT-IR and GC-MS, where the observable contour, specifically the peaks (3690.1 cm^{-1}, 3649.1 cm^{-1} and 3399.3 cm^{-1}) at the region of the FT-IR spectrum of all the upgraded Agbabu bitumen compared with the FT-IR spectrum of the raw Agbabu bitumen were noticed to disappear almost completely, indicating heavy molecular bond breakage to smaller bonds (such as saturates, aromatics and resins in some cases). The GC-MS spectrum of the upgraded Agbabu bitumen showed more chemical compounds available in the upgraded Agbabu bitumen than presented in the GC-MS of the raw Agbabu bitumen. However, this scenario was exceptional in the application of the CoMo/HZSM-5 catalyst for the bitumen upgrade, which has fewer chemical compounds in its GC-MS spectrum of the upgraded Agbabu bitumen and maybe because the CoMo/HZSM-5 catalyst has less pore volume and active sites compared to the other catalysts (NiMo/ZSM-5, and Mo/HZSM-5) employed, with NiMo/ZSM-5 catalysed upgraded Agbabu bituminous crude oil having the most chemical compounds present in its GC-MS spectrum. Also, NiMo/ZSM-5 catalysed upgraded bituminous oil has the API gravity and H/C ratio higher, viscosity, asphaltenes and sulphur contents lower and more produced gas (CH_4 and H_2 gas) compared to the other CoMo/HZSM-5 and Mo/HZSM-5 catalysed upgraded bituminous crude oil.

Funding

This research did not receive any specific grant from funding agencies in the public, commercial, or not-for-profit organisations, except a research stipend allocated for the scholarship awarded to me by the Petroleum Technology Development Fund (PTDF), Nigeria, as a research/project fund allocated for students to carry out and/or support their research (being a Master of Engineering Programme).

Acknowledgement

Yunusa M. Oseni wishes to show his profound gratitude and acknowledge the support from the Petroleum Technology Development Fund (PTDF) organisation, which awarded me a Master of Engineering (M.ENG) scholarship to undergo M.ENG Programme. Notwithstanding, an excellent thanks to the Petroleum Technology Development Fund (PTDF) laboratory at Ahmadu Bello University, Zaria (Nigeria) under the Chairmanship of Baba J. El-Yakub for initiating the research-based 'heavy oil or bitumen upgrading' which calls for this paper article as my co-supervisor. A special thanks go to Umar O. Aroke of Abubakar Tafawa Balewa University, Bauchi (Nigeria), for his tireless efforts as the guide and supervisor in preparing this article as my primary supervisor. Finally, my gratitude also goes to my research team members in persons of Suleiman Yahaya Adamu – a PTDF laboratory attendant and Usman Suleiman Baba – a PhD student in the Department of Chemical Engineering, Ahmadu Bello University, Zaria (Nigeria).

REFERENCES

1. Demirbas, A., Bafail, A., & Nizami, A.-S. (2016). Heavy oil upgrading: Unlocking the future fuel supply. *Petroleum Science and Technology, 34*(4), 303–308. doi: 10.1080/10916466.2015.1136949

2. Spiecker, P. M., Gawrys, K. L., Trail, C. B., & Kilpatrick, P. K. (2003). Effects of petroleum resins on asphaltene aggregation and water-in-oil emulsion formation. *Colloids and Surfaces A: Physicochemical and Engineering Aspects, 220*(1–3), 9–27. doi: 10.1016/s0927-7757(03)00079-7

3. Speight, J. G. (2007). *The chemistry and technology of petroleum* (4th ed.). Boca Raton: CRC Press.

4. Li, J., Wang, X., Tang, X., Zhang, M., Zheng, X., Wang, C., & Tang, Z. (2019). Upgrading of heavy oil by thermal treatment in the presence of alkali-treated Fe/ZSM-5, glycerol, and biomass. *Fuel Processing Technology, 188*, 137–145. doi: 10.1016/j.fuproc.2019.02.010

5. Babaso, P. N., & Sharanagouda, H. (2017). Rice Husk and Its Applications: Review. *International Journal of Current Microbiology and Applied Sciences, 6*(10), 1144–1156. doi: 10.20546/ijcmas.2017.610.138

6. Nandiyanto, A. B. D., Oktiani, R., & Ragadhita, R. (2019). How to Read and Interpret FTIR Spectroscope of Organic Material. *Indonesian Journal of Science and Technology, 4*(1), 97. doi: 10.17509/ijost.v4i1.15806

7. Abdulkadir, I., Uba, S., Salihu A., A., & Almustapha, M. N. (2016). A Rapid Method of Crude Oil Analysis Using FT-IR Spectroscopy. *Nigerian Journal of Basic and Applied Sciences, 24*(1), 47. doi: 10.4314/njbas.v24i1.8

8. Ahmad, I., Sohail, S. M., Khan, H., Khan, R., & Ahmad, W. (2108). Characterisation of Petroleum Crude Oils by Fourier Transform Infrared (FT-IR) and Gas Chromatography-Mass Spectrometry. *Petroleum and Petrochemical Engineering Journal, 2*(2), 1–7.

9. Coates, J. (2000). Interpretation of Infrared Spectra, A Practical Approach. *Encyclopedia of Analytical Chemistry*. doi: 10.1002/9780470027318.a5606

10. Jiang, J., Wang, Q., Wang, Y., Tong, W., Xiao, B., & Xiao, B. (2007). GC/MS Analysis Of Coal Tar Composition Produced From Coal Pyrolysis. *Bulletin of the Chemical Society of Ethiopia, 21*(2). doi: 10.4314/bcse.v21i2.21202

11. Bosio, A., Gianoncelli, A., Zacco, A., Borgese, L., Rodella, N., Zanotti, D., Depero, L. E., Siviero, G., Cinosi, A., Bingham, P. A., & Bontempi, E. (2013). A new nanotechnology of fly ash inertization based on the use of silica gel extracted from rice husk ash and microwave treatment. *Proceedings of the*

Institution of Mechanical Engineers, Part N: Journal of Nanoengineering and Nanosystems, 228(1), 27–32. doi: 10.1177/1740349913490683

12. Treacy, M. M., & Higgins, J. B. (2001). *Collection of Simulated XRD Powder Patterns for Zeolites (*4th ed.). New York: Elsevier.

13. Pavlačková, Z., Košová, G., Žilková, N., Zukal, A., & Čejka, J. (2006). Formation of Mesopores in ZSM-5 by Carbon Templating. *Scientific Bases for the Preparation of Heterogeneous Catalysts*, 905–912. doi: 10.1016/s0167-2991(06)80996-1

14. Yan, Y., Guo, X., Zhang, Y., & Tang, Y. (2015). Future of nano-/hierarchical zeolites in catalysis: gaseous phase or liquid phase system. *Catalysis Science & Technology, 5*(2), 772–785. doi: 10.1039/c4cy01114g

15. Zhang, K., & Ostraat, M. L. (2016). Innovations in hierarchical zeolite synthesis. *Catalysis Today, 264*, 3–15. doi: 10.1016/j.cattod.2015.08.012

16. Fernandez, C., Stan, I., Gilson, J., Thomas, K., Vicente, A., Bonilla, A., & Pérez-Ramírez, J. (2010). Hierarchical ZSM-5 Zeolites in Shape-Selective Xylene Isomerization: Role of Mesoporosity and Acid Site Speciation. *Chemistry – A European Journal, 16*(21), 6224–6233. doi: 10.1002/chem.200903426

17. Chou, Y. H., Cundy, C. S., Garforth, A. A., & Zholobenko, V. L. (2006). Mesoporous ZSM-5 catalysts: Preparation, characterisation and catalytic properties. Part I: Comparison of different synthesis routes. *Microporous and Mesoporous Materials, 89*(1–3), 78–87. doi: 10.1016/j.micromeso.2005.10.014

18. Agliullin, M. R., Talzi, V. P., Filippova, N. A., Bikbaeva, V. R., Bubennov, S. V., Prosochkina, T. R., Grigorieva, N. G., Narender, N., & Kutepov, B. I. (2018). Two-step sol–gel synthesis of mesoporous aluminosilicates: highly efficient catalysts for the preparation of 3,5-dialkylpyridines. *Applied Petrochemical Research, 8*(3), 141–151. doi: 10.1007/s13203-018-0202-0

19. Guo, K., Li, H., & Yu, Z. (2016). In-situ heavy and extra-heavy oil recovery: A review. *Fuel, 185*, 886–902. doi: 10.1016/j.fuel.2016.08.047

20. Scott, D. S., Radlein, D., Piskorz, J., Majerski, P., & deBruijn, Th. J. W. (2001). Upgrading of bitumen in supercritical fluids. *Fuel, 80*(8), 1087–1099. doi: 10.1016/s0016-2361(00)00174-5

21. Ates, A., Azimi, G., Choi, K.-H., Green, W. H., & Timko, M. T. (2014). The role of catalyst in supercritical water desulfurisation. *Applied Catalysis B: Environmental, 147*, 144–155. doi: 10.1016/j.apcatb.2013.08.018

22. Avbenake, O. P., Al-Hajri, R. S., & Jibril, B. Y. (2019). Catalytic upgrading of heavy oil using NiCo/γ-Al2O3 catalyst: Effect of initial atmosphere and water-gas shift reaction. *Fuel, 235*, 736–743. doi: 10.1016/j.fuel.2018.08.074

23. Yusuf, A., Al-Hajri, R. S., Al-Waheibi, Y. M., & Jibril, Baba. Y. (2016). In-situ upgrading of Omani heavy oil with catalyst and hydrogen donor. *Journal of Analytical and Applied Pyrolysis, 121*, 102–112. doi: 10.1016/j.jaap.2016.07.010

24. Kumar, S., & Mahto, V. (2016). Emulsification of Indian heavy crude oil in water for its efficient transportation through offshore pipelines. *Chemical Engineering Research and Design, 115*, 34–43. doi: 10.1016/j.cherd.2016.09.017

25. Li, J., Wang, X., Tang, X., Zhang, M., Zheng, X., Wang, C., & Tang, Z. (2019). Upgrading of heavy oil by thermal treatment in the presence of alkali-treated Fe/ZSM-5, glycerol, and biomass. *Fuel Processing Technology, 188*, 137–145. doi: 10.1016/j.fuproc.2019.02.010